Influence of reduced graphene oxide on epoxy/carbon fibre-reinforced hybrid composite: flexural and shear properties under varying temperature conditions.

JENKINS, P., SIDDIQUE, S., KHAN, S., USMAN, A., STAROST, K., MACPHERSON, A., BARI, P., MISHRA, S., NJUGUNA, J.

2019

Influence of Reduced Graphene Oxide on Epoxy / Carbon Fibre-Reinforced Hybrid Composite: Flexural and Shear Properties Under Varying Temperature Conditions

Paddy Jenkins[1], Shohel Siddique[1], Samrin Khan[2], Aliyu Usman[1], Kristof Starost[1], Allan MacPherson[1], Pravin Bari[2], Satyendra Mishra[2], James Njuguna[1]*

[1]Centre for Advanced Engineering Materials, School of Engineering, Robert Gordon University, Riverside East, Aberdeen, AB10 7GJ, United Kingdom

[2]University Institute of Chemical Technology, North Maharashtra University, Jalgaon - 425001, Maharashtra, India

*Corresponding Author Email: j.njuguna@rgu.ac.uk; Tel. +44 (0) 1224262304

Abstract

This study investigated the effectiveness of reduced graphene oxide as nanofiller in enhancing epoxy/carbon fibre-reinforced composite at varying temperature conditions. The graphene oxide was synthesised using modified Hummer's method and then chemically reduced to yield reduced graphene oxide (rGO). The rGO was dispersed in epoxy matrix system through combination of mechanical and sonication methods. The flexural and shear test samples were manufactured using resin infusion technique. These samples were then tested to determine their shear and flexural properties at varying temperatures (-10 ^{o}C, 23^{o}C, 40 ^{o}C) and the results correlated to neat samples. It was found that the composites' flexural strength and flexural modulus increased with rGO wt.% content up to 62% and 44% respectively. The shear testing results showed improvement on the shear strength and modulus at maximum of 6% and 40% respectively. The rGO improvements advantage was lost for flexural strength, shear strength and modulus at elevated temperatures while flexural modulus withheld at 40% improvements over virgin epoxy/carbon fibre-reinforced composite. An interesting observation is that all samples with rGO exhibite reduced damage characteristics superior to the neat samples under flexural and shear loading conditions. This study indicates that the addition of rGO significantly alter the flexural and shear properties, failure modes, damage characteristics and they are overall sensitive to elevated temperature conditions.

1 Introduction

Epoxy resin is a type of polymer characterized often with one or more epoxide functional group with at least one of the epoxide functional group acting as a monomer and terminal unit of the polymer within the structural chain [1-3]. Epoxy resins are extensively used in the production of lightweight carbon fibre-reinforced composites (CRFP) to deliver desired engineering properties such as high modulus and strength, low creep, superb chemical and thermal stability [4, 5]. The epoxy/carbon fibre-reinforced composite design, just like any other composite, is heavily dependent on the mechanical and thermal properties of the resulting composites of the manufactured epoxy/carbon fibre-reinforced composite withstanding the conditions set by its application requirements.

The mechanical properties such as flexural, tensile and shear strengths respectively cannot be overly emphasized with regards to manufacture design with each material property defined by the type of loading subjected to the epoxy composite in applications. Of particular interest is the effect of temperature changes on mechanical properties that is relevant and specific to applications such as the aerospace, racing cars, marine and automotive industry where temperature changes can vary significantly in lightweight applications [6, 7]. It is well known that temperature can have a significant impact on the shear and flexural strength of composite materials and that the addition of nanofiller may have some effect on how temperature influences strength.

For example, Kichhannagari [8] investigated the effect that changes in temperature had on the shear strength of a plain carbon fibre composite material focusing on the formation of micro-cracking. The investigation reported that shear strength increased with decrease in temperature. The greatest increase of shear strength was found during the temperature transition from 23 ^{o}C down to -100^{o}C. It was reported that the tensile strength of this material followed a similar pattern. Another study used acoustic emission to detect micro cracks in the carbon fibre composite as it experienced temperature changes from 23 ^{o}C down to -100^{o}C and reported that micro cracks can form rapidly with the decreasing temperature and that a positive temperature gradient causes a much slower and almost negligible growth in these cracks [8]. Residual deformation in composites can also be affected by the ambient temperature. Nikolaev [9] found that as the temperature increased, the residual deformation from a variety of loading conditions becomes more apparent.

The addition of nanofillers into the resin system during composite manufacturing can directly influence the mechanical, thermal and chemical properties of the resulting composite. In turn this increase e.g. the strength, dimensional properties and hence extend the functional life of the material although graphene nanofillers remain extremely expensive the addition of small amounts is known to improve the mechanical qualities of a composite [10, 11].

It is acknowledged that the addition of graphene oxide (GO) or reduced graphene oxide (rGO), as nanofiller, to a composite material can increase its strength. This is due to its unique ability to fill in micro-cracks as they form within the material. For instance, Bortz [12] investigated the effect of varying quantities of graphene oxide (GO) on the flexural properties of epoxy/ carbon fibre reinforced composites. The study found that the addition of just a small amount (0.1wt.%) of GO powder can increase the flexural strength by 25%. However, this improvement is not a linear relationship and the continued addition of GO did not increase the strength in the same fashion. The increases in flexural strength between 0.1 wt.% GO and 1 wt.% GO was only found to be roughly 5%. This may be due to the GO causing the resin matrix to become brittle and lack of effect fibre-matrix adhesion. Tribological performance of epoxy nanocomposites was conducted by Shen et al. [13] and reported that the wear resistance is significantly enhanced by the addition of GO to epoxy and the specific wear rate is reduced by over 90% relative to the neat epoxy at 0.5 wt%.GO content. Wan et al [14] studied the epoxy composites filled with both graphene oxide (GO) and diglycidyl ether of bisphenol-A functionalized GO (DGEBA–f–GO) sheets. Han et al [15] studied GO / epoxy fibre reinforced composites achieved the improvements on interlaminar shear strength (ILSS) attributed to better epoxy resin toughness.

The reduction of GO partly restores the structure and properties of graphene is a key topic in the research at present. Different reduction processes result in different properties of reduced GO (rGO), which in turn affect the final performance of materials or devices composed of rGO. Also, nanofilling of rGO to epoxy/carbon fibre nanocomposites is a relatively new approach with a high interest to fibre reinforced composite manufacturing of components due to its potential in properties and performance improvements.

Publications on rGO/epoxy-fibre reinforced composites are scares in the open literature. Further, there are currently limited publications in the open literature on shear properties and thermo-mechanical properties of rGO/epoxy fibre-reinforced composites. Recent efforts focused on Konios [16] studied the dispersion of GO and rGO in various media, Chen et al studied electromagnetic properties [17], cryogenic performance [10, 18], and other researchers on rGO investigated fatigue performance [12]. The utilisation of rGO on composites components depends on full understanding of the mechanical properties and their functional performance. This study therefore focus on the evaluation of epoxy/carbon fibre-reinforced composite containing varying quantities of rGO and examine the shear and flexural properties of these samples at varying temperatures.

2 Experiments

2.1 Materials

The graphene oxide was synthesised using a modified and improved Hummer's method [19]. In a typical synthesis, concentrated H_2SO_4 and H_3PO_4 with a 9:1 mixture (360:40 mL) were added to 3g of graphite powder. 18g of $KMnO_4$ was then added to the mixture under constant magnetic stirring producing a slightly exothermic reaction. In the next step, the reaction was stirred for 12 hours at a constant 50 ^oC followed by cooling to room temperature and then poured onto ice with 30% H_2O_2 (3mL). The mixture was then sifted through a sieve and filtered through polyester fibre. The filtrate was centrifuged, and the supernatant was decanted away. This was followed by washing the solid material with 200mL of water, 200mL of 30% HCl, and 200mL of ethanol twice. For each wash, the mixture was sifted and filtered again before further centrifugation of the filter. The final material remaining was coagulated with 200ml of ether. Further drying yielded graphene oxide for further studies.

To synthesis of rGO, graphene oxide was next chemically reduced further to produce rGO as shown on Figure 1.

Figure 1

In a typical process, the GO and distilled water was taken in 900mg: 900ml ratio and sonicated for 30 min. Then the mixture was transferred into round bottom flask and hydrazine hydrate was added into the mixture and then kept the mixture for 24 hours at 100 °C in an oil bath with mild stirring. The suspension was then settled for 12 hours and followed by washing with water and ethanol and dried for a further 12 hours. Carbon fibre fabric (200gsm, 3K twill) and a two-part epoxy (IN2) and its AT30 hardener (polyoxypropylene diamine) was supplied by Easy Composites Ltd.

2.2 Manufacturing of the test samples

Four sets of samples (with/out) rGO were manufactured for flexural and shear testing using resin infusion technique. The 0.1, 02 and 0.3 wt.% rGO was dispersed in epoxy resin using sonication process in parallel programme as in our previous studies [20-22]. This was achieved by sonicating

the rGO powder in acetone for a 30 minute before this acetone/rGO solution was then mechanically mixed into the epoxy resin for a further 30 minutes. The resin/acetone solution was then sonicated at 60^{o}C for 5 hours to ensure effective dispersion of the rGO whilst also removing the acetone by evaporation. Once all traces of acetone were removed from the epoxy/rGO solution by drying at 80^{o}C in a vacuum oven for 12 hours, then addition of the hardener and infusion process were carried out as normal. A 60:40 fibre-epoxy volume ratio and epoxy resin to hardener (100:30) was employed as recommended by the supplier. The mixture was next dried in a vacuum chamber for 10 minutes to remove air bubbles before vacuum infusion process.

The composite plates for flexural testing with a thickness of 4 mm, 16 layers and the weave running at 0^{o}/90^{o} were manufactured to produce samples for testing under the standard ASTM D7264 (4 point bend) [23]. The second set of plates for shear testing made of 12 plies laid up at 0^{o} / 90^{o} 3 mm thick were also separately manufactured using resin infusion. The samples were left to cure for 48 hours before being removed from the vacuum bags. The peel ply was later removed along with the infusion mesh and connectors to leave solid composite plates. Neat samples (without rGO) were also manufactured using the resin infusion for reference purposes. The respective plates were then machined using a diamond cutter to produce flexural and shear test specimens meeting the ASTM D7264 [23] and ASTM D7078 [24] test standards respectively.

2.1 Characterisation

The surface morphology of the epoxy nanocomposites was examined using a scanning electron microscope (SEM) (S4800, Type II, Hitachi, Tokyo, Japan) at an operation voltage of 10 keV and a pressure of 0.98 Torr. The epoxy nanocomposite specimens were coated with gold and mounted on the specimen stub before analysis. The post-testing samples were observed using a Zeiss EVO LS10 SEM with a magnification of 4.5 mm working distance (WD) and accelerating potential of 25.00kV. To minimise the sample being altered all the samples are gold coated using sputter deposition for 2 minutes prior to the experiment.

Samples of the GO and epoxy nanocomposites were finely divided and dispersed in a KBr powder for analysis for Fourier transform infrared (FTIR) spectroscopy. The FTIR spectrophotometer (8400, Shimadzu, Tokyo, Japan) was used to obtain spectra and to comprehend the bond formation between filler and epoxy resin. Total 45 scans were taken for each nanocomposite sample recorded at 4000–400 cm^{-1} with resolution of 4 cm^{-1} in the transmittance mode.

Thermogravimetry analysis (TGA) was carried out using a TA Q500 instrument to determine the degradation and decomposition temperature as well as the rate of degradation of the nanocomposite samples. This analysis is performed by measuring the weight variation of a given sample due to temperature increase and phase change as the sample degrades until it is decomposed. The TGA instrument used is TA instrument Q500. The temperature is being set on ramp mode from room temperature (20 ºC) to 1000 ºC at a rate of 10 ºC per minute.

Differential Scanning Calorimetry (DSC) analysis is was performed with a TA Q100 instrument under a nitrogen environment to ascertain the melting temperatures, crystallisation temperatures as well as the glass transition temperatures of the materials. The instrument measured the differences in heat exchange between the sample and the reference (an empty aluminium pan). The DSC instrument used is TA instrument Q100. The temperature being set on heat/cool/heat procedure or mode from a temperature of -20 ºC to 250 ºC at a rate of 10 ºC per minute.

2.2 Testing

All tests were carried out using an Instron 3382 universal testing machine equipped with an environmental chamber and using Bluehill software. The load was measured using a 100kN load cell. The experiments were conducted according ASTM D7264 (4-point bending) [23] with samples diameter as 154 mm x 13 mm x 4 mm. The shear testing was carried out under ASTM D7078 (V notched) [24] as shown on Figure 2 with samples dimensions as 76 mm x 56 mm x 3 mm.

Figure 2

Five samples of each size at each reference (neat) samples and for each concentration of rGO were manufactured and tested at crosshead speeds 2 mm/min (flexural), 0.5mm/min (shear) and at three different temperatures at -10ºC, 23 and 40ºC (flexural) and at 23 and 40ºC (shear) to evaluate how these materials may perform under various operational environments for automotive exterior structural components.

3 Results and Discussion

3.1 Morphology studies

The morphology and structure of GO and RGO nanosheets were investigated through FE-SEM. Figure 3(b) presents the representative FE-SEM image of free-standing GO nanosheets, revealing a crumpled and rippled structure which was the result of deformation upon the exfoliation and restacking processes [25, 26]. The rGO nanosheets, however, are layer structured, irregular and folding, as shown in the SEM image of Figure 3(b). Figure 3(c) exhibits TEM morphology of the GO, shows a wrinkled surface which provides stability and prevents collapse back to a graphitic structure [27, 28]. Significant structural changes occur during the chemical processing from GO to rGO nanosheets, which have also been characterized by Raman spectroscopy as shown in Figure 4.

Figure 4

Detailed morphology studies and characterisation of GO used in this study are available in our previous works [20]. From Figure 4, the characteristic peaks for graphite ca. 1600 cm^{-1} (G-band) and 1350 cm^{-1} (D-band) are observed. G-band is due to sp^2-hybridized carbon network originated from the first-order scattering of doubly degenerate E_{2g} phonon modes of graphite in the Brillouin zone centre; while D-band is for structural imperfections due to the attachment of oxygenated groups on the carbon basal plane [29, 30]. The intensity ratio of D-band and G-band (ID/IG) is used for prediction of sp^2 network size and defects in GO and rGO [31]. In this case, the D/G intensity ratio of GO (ID/IG) is 1.05, slightly smaller than that of RGO (ID/IG=1.22), confirming that more defects are induced in the rGO during the reduction process.

Figure 5

Figure 5 shows that GO has peaks at 1061 cm^{-1} and 1730 cm^{-1} which are attributed to the C-O and C=O bond respectively, confirming the presence of oxide functional groups after the oxidation process. The peaks in the range of 1630 cm^{-1} to 1650 cm^{-1} show that the C=C bond remained after the oxidation process. The absorbed water in GO is shown by a broad peak at 2885 cm^{-1} to 3715 cm^{-1}. In rGO, the peaks at 1061 cm^{-1} and 1730 cm^{-1} get completely disappeared, confirming the removal of oxygenated groups during the reduction process [31, 32]. The peak at 1530 cm^{-1} corresponds to

C=C bond. So from the FTIR data, simultaneous oxidation and reduction of GO and rGO is confirmed [30, 33].

3.2 Thermal properties

Thermal properties were investigated using TGA and DSC techniques. The TGA results in Figure 6 (a) shows decreasing trend of thermal decomposition of materials with the incremental addition of rGO to the sample, which implies that the char formation increases with the incremental increases of rGO content in hybrid nanocomposites.

Figure 6

Glass transitional temperature, T_g, is a very vital thermal property that governs the material characteristics of a polymer/composite; particularly thermosets, within a defined temperature regime owing to their amorphous nature [6]. Considering onset degradation at 5 wt.% ($T_{d5\%}$) in Figure 6(b) and onset degradation between 250-450° C (major decomposition stage) in Fig. 2(c), it can be attributed that addition of rGO significantly increases the thermal stability of hybrid nanocomposites. In Figure 6(b), epoxy with 0.2 wt% rGO shows the highest onset degradation temperature which is 12.33° C higher than that of neat epoxy. In addition, in Figure 6(c), epoxy with 0.3 wt% rGO shows the highest onset degradation temperature (313.59° C) which is 16.5° C higher than that of neat epoxy. Observing the thermograms in Figure 6(b), it can be manifested that the time needed to reach 50 wt% decomposition of neat epoxy and epoxy hybrid nanocomposites is not been hindered due to the presence of rGO which implies rGO does not have any significant flame-retardant effect on that polymer matrix

From the DSC results, the corresponding T_g, T_m and region of operation before complete thermal failure of the samples are illustrated on Table 1 and Figure 7.

Table 1

Figure 7

It is observed that initially the T_g is close to the room temperature possibly as a result to the samples being cured room temperature. In addition, it is also observed that addition of rGO does not affect the glass transition temperature of epoxy with 0.1 wt.% and 0.2 wt.% rGO. However, the glass

transition temperature is reduced by more than 46% with the 0.3 wt% addition of rGO with epoxy. However, an increase of T_m in 0.1 wt.% rGO and 0.2 wt.% rGO samples followed by a sharp decline of T_m in 0.3 wt.% rGO sample was observed on the exotherm plots. In comparison to the neat variant of the sample, it was noted that the 0.2 wt.% rGO sample exhibited superior thermal stability with regards to thermal degradation upon application of a thermal load with a thermal window of operation of 60.73°C before the matrix begins to melt leading to the compromise of its mechanical ability compared to the other incremental variations of the sample.

3.3 Flexural Properties

Flexural properties are prominent and vital mechanical property of materials particularly in composites and is referred to among others the ability of a material to withstand failure from bending forces. Figure 8 shows the results the 4-point bending test at room temperature for neat 0.1 wt.%, 0.2 wt.% and 0.3 wt.% content of rGO samples.

Figure 8

The results show that the addition of rGO increased epoxy/carbon fibre-reinforced composites ability to resist deformation under exerted load at the expense of brittleness. The failure may be induced by poorly dispersed rGO causing brittle areas in the samples tested. The 0.2% and 0.3% samples had higher flexural moduli and flexural stiffness respectively than the neat samples. For example, adding 0.2% weight of rGO to the epoxy improved maximum stress and failure load compared to the samples with neat epoxy resin.

Results from low temperature (-10^{o}C) flexural studies are shown Figure 8(i). A similar performance to the room temperature testing with the samples containing rGO generally sustaining higher stress performance levels than reference composite. The rGO content did not seem to be affected by the lower temperature and led to the flexural strength increase by similar level to the room temperature (Figure 8(ii)) test results. It is normally expected that the colder temperature would affect the epoxy in such a way that the composite would become more brittle and, while this was shown to be true for the neat samples, the samples containing 0.2 and 0.3% rGO did not seem to be affected in the same way by the colder temperatures. This indicated that the addition of rGO nanofiller may be useful for combating the mechanical issues presented by an epoxy/carbon fibre composite at low temperatures.

High temperature testing was carried out at 40^{o}C and results presented Figure 8(iii). Again, the samples show increasing flexural strain for all samples tested and with no clear yield point or fracture point. During testing these samples continued to deform at a relatively steady rate and, for this reason,

graphs produced only show up to a strain of 0.014 mm/mm. After this point samples continued to deform without snapping or breakage. Although the glass transition temperature of the epoxy is 60 ^{o}C mentioned in literature [34], the composites analysed in this study significantly lost rigid properties at much lower temperatures i.e. 24 ^{o}C. It should be noted that the glass transitional temperature of a thermoset is referred to as the temperature or temperature range whereby a thermoset shifts its mechanical behaviour from a rigid and glassy state to a more flexible and rubbery state.

T_g is heavily dependent on the type and temperature of curing employed for the manufacturing process of the thermoset. As such, T_g governs the mechanical properties at given temperature regime, in which the basis of operations is carried out under the limit to avoid accidents associated with change in mechanical behaviour. Figure 9 clearly shows the flexural performance comparison of samples containing rGO wt.% content at differing temperatures.

Figure 9

It can be observed that at all percentage quantities of rGO show the same trends of increasing flexural strength with decreasing temperature. Neat, 0.1%, 0.2% and 0.3 wt.% rGO quantity samples show very similar trends with samples tested at room temperature and -10^{o}C being very close in gradient and maximum stress although colder temperature samples produce slightly higher maximum stress and the main difference is the maximum strain. At colder temperatures samples can withstand lesser strain and brittle. The 0.1 wt.% rGO samples show much greater difference between room temperature and cold temperature results with the colder temperature giving almost 30MPa higher flexural stress than those tested at room temperature. This may be due to the colder temperature reducing the effect that the poorly dispersed rGO had on the overall properties of the samples as observed on scanning electron microscopy images.

Samples tested at higher temperatures showed consistently lower flexural strength with samples generally being unable to withstand more than 100MPa stress with exception of the 0.3 wt.% rGO samples. The 0.3 wt.% rGO samples were able to withstand 110MPa, indicating that even when the epoxy is beginning to lose its rigidity due to increased temperature, the rGO is still able to have a role in influencing on the mechanical properties. The results show the expected trends of increasing flexural strength when more significant quantities of rGO are added or temperature is reduced except for the 0.1wt.% samples. The results show similar performance to a similar investigation conducted on the addition of GO to a composite [12]. Overall, the flexural test results at a lower temperature (-10^{o}C) showed improved results all round due to the lower temperatures giving the epoxy a higher flexural modulus therefore increasing the flexural modulus of the whole composite. The additions of rGO gave improved flexural properties in the higher two out of the three concentrations.

Flexural testing (4-point bending) results (Figure 10) showed drastic improvement in the flexural strength of the samples and flexural modulus of the material across all three temperatures investigated when 0.2 wt.% rGO and 0.3 wt.% rGO was dispersed in the epoxy before infusion.

Figure 10

Although these samples with added nanofiller were shown to be slightly more brittle than the neat composite, an average 0.3% sample was able to withstand close to 75 MPa higher stresses than a neat sample. This improvement in flexural properties far outweighs the slight reduction in the material's ductile abilities. Results of flexural strength and modulus for 0.1% rGO showed a reduced ability to withstand flexural loading, showing brittle tendencies when compared to the neat samples. The poor performance of the 0.1 wt.% rGO samples was assumed to be due to defects experienced during the manufacturing stage although advantageous in shear performance as noted later. This indicates that the addition of rGO as a nanofiller can significantly alter the flexural properties of the composite and therefore more caution is required when designing such composites.

3.4 Shear Properties

The shear testing focused on the composite's performance at room temperature and at 40^{o}C. The results of shear stress and strain are shown in Figure 11.

Figure 11

The 0.2% samples generally showed the lowest shear strength, samples generally failing between 72 and 75 MPa although one sample was able to withstand nearly 100 MPa. The neat samples recorded the lowest performance failing approximately between 75-85 MPa. The 0.3% samples gave a much more consistent performance result with low standard deviation. However, these samples with the highest percentage content of rGO proved not to be the strongest samples with the 0.1% samples clearly being stronger where two of the samples withstood roughly 100 MPa.

Neat samples and 0.3% samples showed the most ductile properties, withstanding large amounts of strain, over 0.14 mm/mm. whereas 0.1% and 0.2% samples failed close to 0.08 mm/mm of strain. Neat samples show a similar gradient to all other samples until a strain of 0.02 mm/mm is reached, after this the gradient reduces as the sample begins to plastically deform and the stress continues to increase until it reaches a maximum of 78 MPa at 0.11 mm/mm. After this point the sample continues to plastically deform with the stress not falling dramatically.

The 0.3% samples show a similar trend with a continually decreasing gradient up to a maximum stress of 88 MPa at 0.11 mm/mm. Again, the sample continues to plastically deform after this point although it does not completely fracture as there is still significant stress experienced. As mentioned previously, the 0.2 wt.% and 0.1 wt.% rGO samples show a steeper gradient as they reach maximum stress at a much lower strain that the other samples - both reaching maximum stresses just below 0.08 mm/mm strain, the 0.2% sample fails at 74 MPa while the 0.1% sample reaches 100 MPa. It is expected that the samples only fracture when fibre-matrix bonding begin to break and, due to the nature of the test, it can therefore be eluded that enough fibres did break to cause fracture. Neat and 0.3 wt.% rGO samples failed but did not experience fracture whereas 0.1 wt.% and 0.2 wt.% rGO samples failed and fractured at similar points and manner. These shows the 0.1 wt.% and 0.2 wt.% rGO samples are more brittle compared to the neat and 0.3% samples that showed more ductile properties.

As the epoxy began to crack, the fibres could move and continue to hold the sample together therefore keeping a relatively constant stress within the material as similarly reported in the literature [15]. The 0.1 wt.% rGO samples had notable poor dispersion and the agglomerate of rGO may have restricted any movement by the fibres causing a brittle failure. Further, the larger rGO clusters may have also increased the shear strength of the sample by giving it rigid properties and enabling it to resist the shear force applied during the test more successfully than well dispersed rGO samples. The 0.3 wt.% rGO samples also failed without fracturing to a noticeable degree. These samples contained the highest quantity of rGO and, as rGO is a form of graphite, and it has good lubrication properties, this may have allowed the plies to slide against each other after failure which would have resulted in the increased strain experienced without the material fracturing. It is also taken that the 0.2 wt.% samples contained a smaller quantity of rGO which may not have allowed plies to slide a possible explanation of the sudden failure at a low strain and stress value.

According to Griffith crack theory, all materials contain small cracks due to production defects, but these cracks will not grow (propagate) until high enough stresses are sustained in the component. Considering this, it can be assumed that all samples contained cracks although samples that failed prematurely must have contained larger cracks which required lower stresses in order to propagate as noted by Maleque [35] that rGO in these samples was also better dispersed meaning that larger agglomerates would have been rare, meaning any benefit that these clumps had in preventing fracture as they did in the 0.1 wt.% rGO sample would have been limited.

Figure 11 shows the results of shear testing at 40^{o}C. As was shown in the flexural results, the higher temperature caused the epoxy to become malleable as it was close to its glass transition temperature. This gave lower performance results as was the case with the flexural testing at the same temperature,

it was therefore assumed that the early elastic-plastic transition was due to the epoxy resin coming close to its glass transition temperature.

Generally, all samples show a similar gradient up until a strain of 0.05, exceptions are the neat samples which seem to show a random result. The other two neat samples show both more defects in the sample leading to reduced load being applied, potentially due to a more ductile or brittle sample therefore showing greater extension at a lower load or vice versa. From these results at 40^{o}C, it may be suggested that although the addition of rGO does not significantly improve the shear strength of the samples, it does give the material more consistent mechanical properties therefore reducing the chance of premature failure.

Overall, the shear testing study of all samples showed a similar gradient up to 0.05 mm/mm of strain. After this point the trends diverge depending on the rGO wt.% content. The 0.2% samples begin to plastically deform first, failing close to 45 MPa at a strain of 0.14. Next to fail are the 0.1% and 0.3% rGO samples failing at 47 MPa and 52 MPa respectively. The 0.3% rGO sample experiences the highest strain before failure, extending by up to 6 mm/mm, whereas other samples did not extend much more than 4.5 mm/mm. Neat samples performed relatively well in comparison with samples withstanding roughly 54 MPa stress level, although as with all samples at this temperature, plastic deformation was induced early meaning that the material lost its original shear strength properties at early stages of the testing as illustrated on Figure 12.

Figure 12

For all cases the higher temperature reduced the samples' shear strength by over 30%. The most significant reduction in strength, due to increased temperature, was experienced by the 0.1wt.% rGO samples. This may be due to the poor quality of rGO related with the dispersion level allowing the ductile epoxy plies to slip over each other therefore not allowing the sample to withstand the load. It is assumed that the rGO was not significantly affected by the temperature change and all reductions in shear strength were due to the ductile-brittle transition of the epoxy at this temperature.

The shear modulus of the samples follows a similar trend to that of the shear strength in some ways. Again the 0.1% samples show the best performance at both temperatures although the improvement from the neat samples is far less at a higher temperature than it is at room temperature. Generally, samples tested at 40^{o}C gave a modulus value of roughly half those tested at room temperature, although the 0.1 wt.% rGO samples experienced a reduction in shear modulus of nearly 1 GPa from 1.6 GPa to 0.65 GPa. This does not show the same trend in the shear strength reduction from the increase in temperature and is due to the way in which the samples reacted to the loading. When heated, samples generally withstood 30% lower load although the strain caused by these loads does

not affect the stress value. To calculate the modulus, strain is taken into account along with stress, therefore if a sample withstood 30% less load but at a much greater strain.

Unlike the flexural results, the shear testing results did not show significant improvement in properties the composites. Nevertheless, minor improvements were observed for the 0.3 wt.% rGO samples which were able to withstand a higher stress at the same strain as a neat sample and 0.1 wt.% rGO samples which withstood a much higher stress but became brittle failing at a much lower strain. However, the 0.2 wt.% rGO samples showed worse results than the neat samples. This is unlikely to be due to the sample manufacturing process as the flexural samples were produced using the same materials and method.

Shear test results at room temperature found minimal increase in shear strength or modulus for samples containing 0.2 wt.% rGO and 0.3 wt.% rGO when compared to the neat samples. Surprisingly the 0.1 wt.% rGO samples, which were assumed to be flawed due to manufacturing defects, showed a remarkable increase in shear strength and shear modulus (average of 40%) of the samples. It was considered that the larger particle size of the poorly dispersed rGO has reduced the ability of the plies to slide and therefore giving the material the ability to resist shear deformation to a greater degree than samples with well dispersed or without rGO (neat). Further investigations are underway to understand this phenomenon.

3.5 Damage Analysis

The damage characterisation was conducted according ASTM D7264 failure codes [23]. The photographs and micrographs of the failed samples show a good comparison between the samples which failed at high and low temperatures. For flexural results, it can be seen form Figure 13 that at -10^{o}C, fully fractured leaving splintered ends and a crack formation at the v-notch in centre of the sample.

Figure 13

Whereas the sample tested at 40 ^{o}C bent (no visible breakage) as the sample bent, the top plies were forced together causing them to buckle up and fracture due to compression. It is assumed that the plies were able to slide over each other in the high temperature testing meaning that the bottom plies did not experience enough tension to cause any visible damage.

This contrasts with the cold sample where all plies fractured due to tension experienced on the bottom plies and compression experienced on the top plies. All the -10^{o}C and room temperature samples

failed in similar fashion (fractured) with the most noticeable difference between cold/room temperature and hot temperatures. The cold samples generally failed due to tension and compression at various points across the cross section between the two loading points. Conversely, the 40 ^{o}C tests, the top side of the samples failed due to buckling close to the loading point.

Figure14 shows typical two samples which failed at high and low temperatures this time with high rGO content.

Figure 14

As with the samples containing no rGO (neat), the cold sample experienced a more brittle fracture shown by the cross ply and inter laminar damage. This sample did not break completely but instead the lower plies broke under tension while there was inter laminar failure in the middle section of the sample. This left a few plies on the top holding the two parts together which was thin enough to allow flexibility of the sample therefore giving the impression of full failure. The sample on the right which experienced loading under an increased temperature can again be seen to have not failed at all. The top plies buckled up at the point of loading while the centre of the sample did not experience much deformation at all.

It was noted that as the load was removed the sample sprung back slightly indicating that although the high temperature reduced the yield point significantly, it did still experience slight elastic deformation along with the more noticeable plastic deformation. Figure 14 shows an overhead view of several failed shear samples; 0.1 wt.% rGO sample and 0.3 wt.% rGO sample tested at room temperature at 40 ^{o}C. The sample tested at a high temperature (Figure 13) shows limited signs of damage, this is due to the malleable epoxy allowing the fibres to deform without breaking. It can be seen by the light reflecting off the surface that it is no longer smooth due to fibres that have moved during the test. The 0.3 wt.% rGO samples show considerable deformation due to the high strain experienced. As the high content of rGO allowed the plies to move with more ease, the epoxy began to crack along with the fibres resulting in the top plies deforming outwards and creating visible ridges and cracks. The 0.1 wt.% rGO sample shows less sign of damage although a few small splits from deformation can be seen down the centre however this sample yielded before the strain reached a point at which plies began to rupture.

The shear fractured samples were further studied using SEM with the specified area of focus at v-notch grove of tested samples. On closer inspection of fractures broken disorientated fibre strands as well as a 4.2 µm transverse gap within the second fracture are seen indicating heavily poor fibre-matrix interaction and matrix debonding on the surface of the composite sample (Figure 15). The matrix-fibre cluster beneath the fractures showed more pronounced debondiing.

Figure 15

For the 0.1 wt.% rGO samples on Figure 15(i), multiple longitudinal micro crack propagations longer than the ones present on the neat sample are seen on the surface morphology of the sample matrix as well as initiation stage of matrix debonding on the lower right corner of the sample at x 100 magnifications are seen. At the area around a micro crack, broken fibre strands and dust particles are littered on the matrix indicating multiple fibre damage and an expanding matrix damage around the micro crack location. Severe fibre breakage and matrix debonding indicative of filler embrittlement as compared to the neat was also observed.

From Figure 15(b), multiple micro crack propagations are seen around the 0.2 wt.% rGO samples' matrix and there are three distinct longitudinal fractures with the left fracture 12.5 µm apart from the site of the middle fracture, and correspondingly, the middle fracture is 43.75 µm away from the fracture on the right indicating a poor matrix loading. Further studies showed a cluster of broken fibre strands and slight matrix crystallization as a result of the nanofiller embrittlement. As seen from Figure 15(d) for 0.3 wt.% rGO, a few broken fibre strands and fewer sites of micro crack propagation are seen compared to the other three samples, few broken fibre strands and a rather crystallized matrix, a significant area of the matrix is compromised and the fibres within the matrix are exposed indicative of matrix debonding.

Comparing the observations of the respective samples, 0.3 wt.% rGO sample showed fewer fibre breakage and longitudinal micro crack propagation and fractures compared to the rest of the sample. However, the same 0.3 wt.% rGO sample experienced heavy crystallization within the matrix compared to the other samples, followed by 0.2 wt.% rGO sample, which indicates the brittle effect of the added filler. As such, the 0.1 wt.% rGo sample exhibited the overall best characteristics, with its behaviour superior to the neat and having no signs of matrix crystallization, hence, exhibiting a better behaviour towards shearing loads.

4 Conclusions

The aim of this study was to investigate the effectiveness of reduced graphene oxide as nanofiller in an epoxy/carbon fibre reinforced composite. Shear and flexural properties were experimentally determined through testing under various temperature conditions. The flexural testing at an increased

temperature (40°C) significantly reduced the load at which the composite samples failed. In contrast, the samples did not fail in the same fashion as when tested at lower temperatures. The material permanently bent rather than snapping and flexural modulus reduced by roughly 60% across all concentrations of rGO. Shear testing at a higher temperature showed reduced performance all round due to the epoxy failing as it had reached its ductile-brittle transition. This was reinforced by microscopy which showed deformed but sparse broken fibres, proving that the material had not fully fractured under the load. The investigation also found that the addition of this nanofiller did not improve the shear properties of the material although it was considered that the filler agglomerates aided shear performance. As predicted, the higher content of rGO made the material more brittle.

Overall it can be concluded that the addition of rGO as a nanofiller would significantly benefit composite components which are required to resist large flexural forces whilst component mass and volume must be kept to a minimum. The composite has been proven to support relatively high applied loads from -10°C up to room temperature and is assumed that the flexural and shear modulus decreases as temperature and ductility increase up to 40°C. Further investigations are underway improve these properties and to evaluate the effect on high strain rate and thermal cycling for various rGO weight fractions.

Acknowledgments

Authors are thankful to DST, Govt. of India and UKIERI, British Council for providing financial assistance to carry out this research work on a research project titled 'Structural Reinforcement and Improvement of Compressive Strength after Impact (CIA) in Hybrid Graphene Nanocomposites', Project No. DST/INT/UK/P - 108/2014). The authors would also like to thank Mr David Smith of School of Engineering for his help in samples machining.

References

[1] H. Miyagawa, M. J. Rich, L. T. Drzal, *Journal of Polymer Science, Part B: Polymer Physics.* **2004,** 42, 4391.

[2] F. H. Gojny, M. H. G. Wichmann, U. Köpke, B. Fiedler, K. Schulte, *Composites Science and Technology.* **2004/11,** 64, 2363.

[3] D. C. Lee, L. W. Jang, *J Appl Polym Sci.* **1998,** 68, 1997.

[4] D. Quan, J. L. Urdániz, A. Ivanković, *Mater Des.* **2018,** 143, 81.

[5] J. Njuguna, K. Pielichowski, J. R. Alcock, *Adv Eng Mater.* **2007,** 9, 835.

[6] Pielichowski K, Njuguna J. *Thermal degradation of polymeric materials.* iSmithers Rapra Publishing; 2005.

[7] Njuguna J. *Lightweight composite structures in transport: design, manufacturing, analysis and performance.* Woodhead publishing; 2016.

[8] S. Kichhannagari, Effects of Extreme Low Temperature on Composite Materials. University of New Orleans Theses and Dissertations. 165**, 2004.**

[9] V. Nikolaev, E. Myshenkova, V. Pichugin, E. Sinitsyn, A. Khoroshev, *Inorganic Materials.* **2014,** 50, 1511.

[10] Y. He, S. Yang, H. Liu, Q. Shao, Q. Chen, C. Lu, Y. Jiang, C. Liu, Z. Guo, *J Colloid Interface Sci.* **2018,** 517, 40.

[11] Dasari A, Njuguna J. *Functional and Physical Properties of Polymer Nanocomposites.* John Wiley & Sons; 2016.

[12] D. R. Bortz, E. G. Heras, I. Martin-Gullon, *Macromolecules.* **2011,** 45, 238.

[13] X. Shen, X. Pei, S. Fu, K. Friedrich, *Polymer.* **2013,** 54, 1234.

[14] Y. Wan, L. Tang, L. Gong, D. Yan, Y. Li, L. Wu, J. Jiang, G. Lai, *Carbon.* **2014,** 69, 467.

[15] X. Han, Y. Zhao, J. Sun, Y. Li, J. Zhang, Y. Hao, *New Carbon Materials.* **2017,** 32, 48.

[16] D. Konios, M. M. Stylianakis, E. Stratakis, E. Kymakis, *J Colloid Interface Sci.* **2014,** 430, 108.

[17] J. Chen, J. Wu, H. Ge, D. Zhao, C. Liu, X. Hong, *Composites Part A: Applied Science and Manufacturing.* **2016,** 82, 141.

[18] Y. Wu, M. Chen, M. Chen, Z. Ran, C. Zhu, H. Liao, *Polym Test.* **2017,** 58, 262.

[19] D. C. Marcano, D. V. Kosynkin, J. M. Berlin, A. Sinitskii, Z. Sun, A. Slesarev, L. B. Alemany, W. Lu, J. M. Tour, *ACS nano.* **2010,** 4, 4806.

[20] P. Bari, S. Khan, J. Njuguna, S. Mishra, *International Journal of Plastics Technology.* **2017,** 21, 194.

[21] Watson G, Starost K, Bari P, Faisal N, Mishra S, Njuguna J. IOP Conference Series: Materials Science and Engineering. IOP Publishing; 2017:012009.

[22] P. S. Khobragade, D. P. Hansora, J. B. Naik, J. Njuguna, S. Mishra, *Polym Int.* **2017,** 66, 1402.

[23] ASTM International. *Standard test method for flexural properties of polymer matrix composite materials.* ASTM International; 2007.

[24] ASTM D7078/D7078M-12. Standard test method for shear properties of composite materials by V-notched rail shear method. In: Anonymous ASTM West Conshohocken, PA; 2012.

[25] C. Fu, G. Zhao, H. Zhang, S. Li, *Int.J.Electrochem.Sci.* **2013,** 8, 6269.

[26] D. Hansora, N. Shimpi, S. Mishra, *Rsc Advances.* **2015,** 5, 107716.

[27] Hansora DP, Mishra S. *Graphene Nanomaterials: Fabrication, Properties, and Applications.* Pan Stanford; 2017.

[28] L. Ramos-Galicia, L. Mendez, A. L. Martínez-Hernández, A. Espindola-Gonzalez, I. Galindo-Esquivel, R. Fuentes-Ramirez, C. Velasco-Santos, *International Journal of Polymer Science.* **2013,** 2013, .

[29] D. Yang, A. Velamakanni, G. Bozoklu, S. Park, M. Stoller, R. D. Piner, S. Stankovich, I. Jung, D. A. Field, C. A. Ventrice Jr, *Carbon.* **2009,** 47, 145.

[30] R. Jain, S. Mishra, *RSC Advances.* **2016,** 6, 27404.

[31] F. Ban, S. Majid, N. Huang, H. Lim, *Int.J.Electrochem.Sci.* **2012,** 7, 4345.

[32] T. Noguchi, M. Sugiura, *Biochemistry.* **2002,** 41, 2322.

[33] S. Park, J. An, R. D. Piner, I. Jung, D. Yang, A. Velamakanni, S. T. Nguyen, R. S. Ruoff, *Chemistry of materials.* **2008,** 20, 6592.

[34] J. Zhou, J. P. Lucas, *Polymer.* **1999,** 40, 5505.

[35] Maleque MA, Salit MS. *Materials selection and design.* Springer; 2013.

Caption of Figures and Tables

Tables

Figures

Table 1 Thermal properties for rGO composites studied

rGO Composition	Tg (° C)	Tm(° C)	Tm-Tc (° C)
Neat	24.43	92.40	70.21
0.1%	24.95	94.99	71.75
0.2%	24.43	92.60	69.98
0.3%	13.07	83.91	61.50

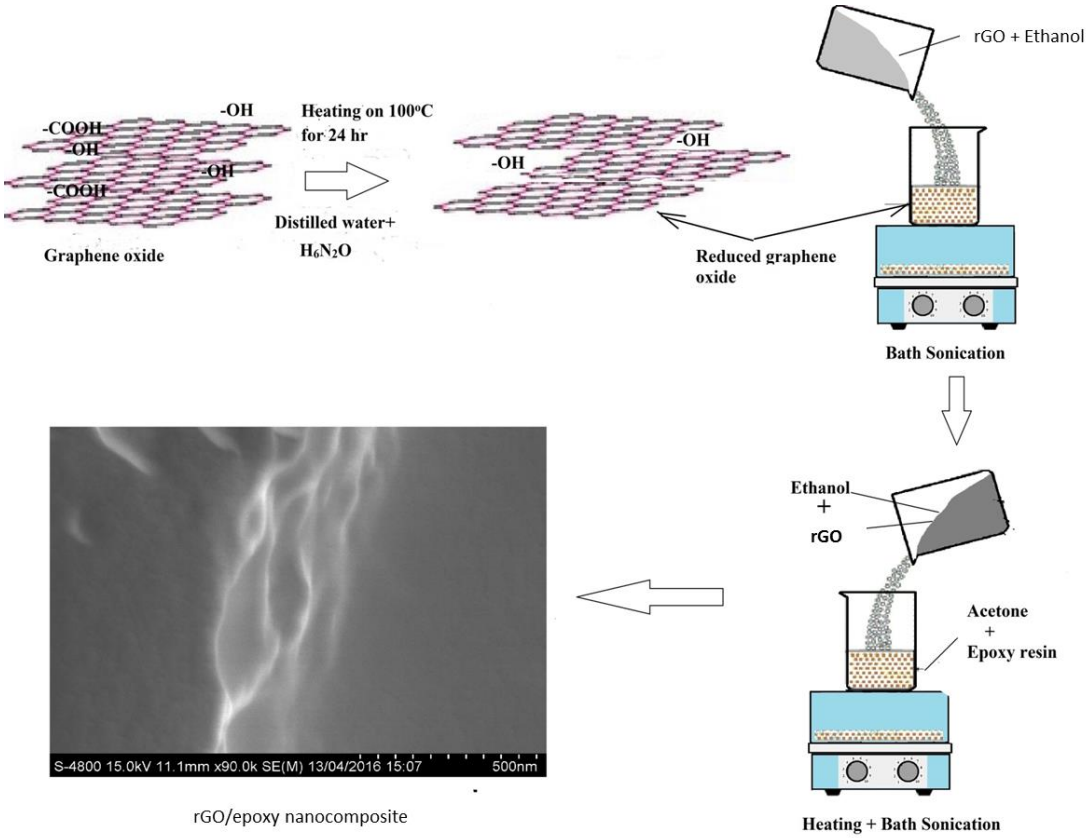

Figure 1 Schematic diagram of graphene oxide to rGO and epoxy / rGO composite

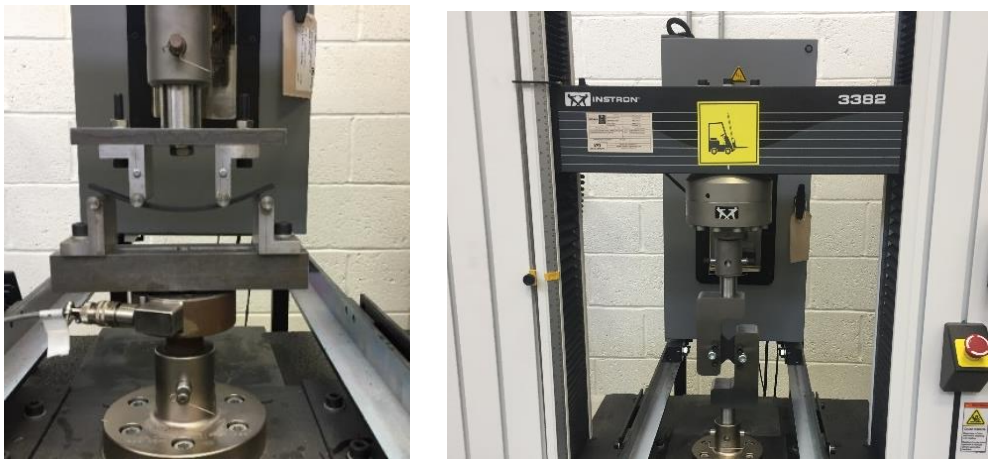

Figure 2 Flexural sample under loading conditions (left) and shear test sample in fixture (right

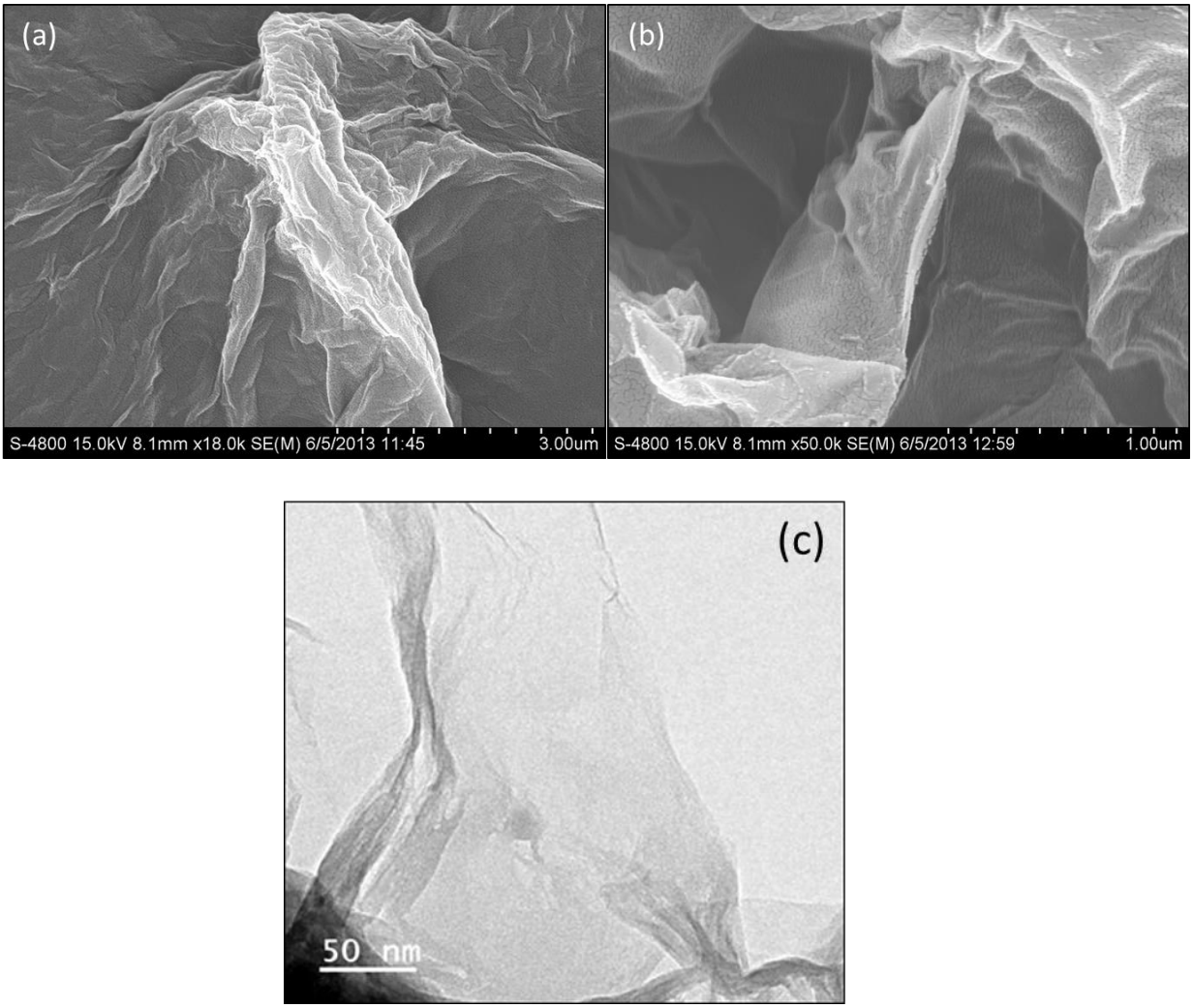

Figure 3 FESEM image of (a) GO and (b) rGO and TEM image of GO (c).

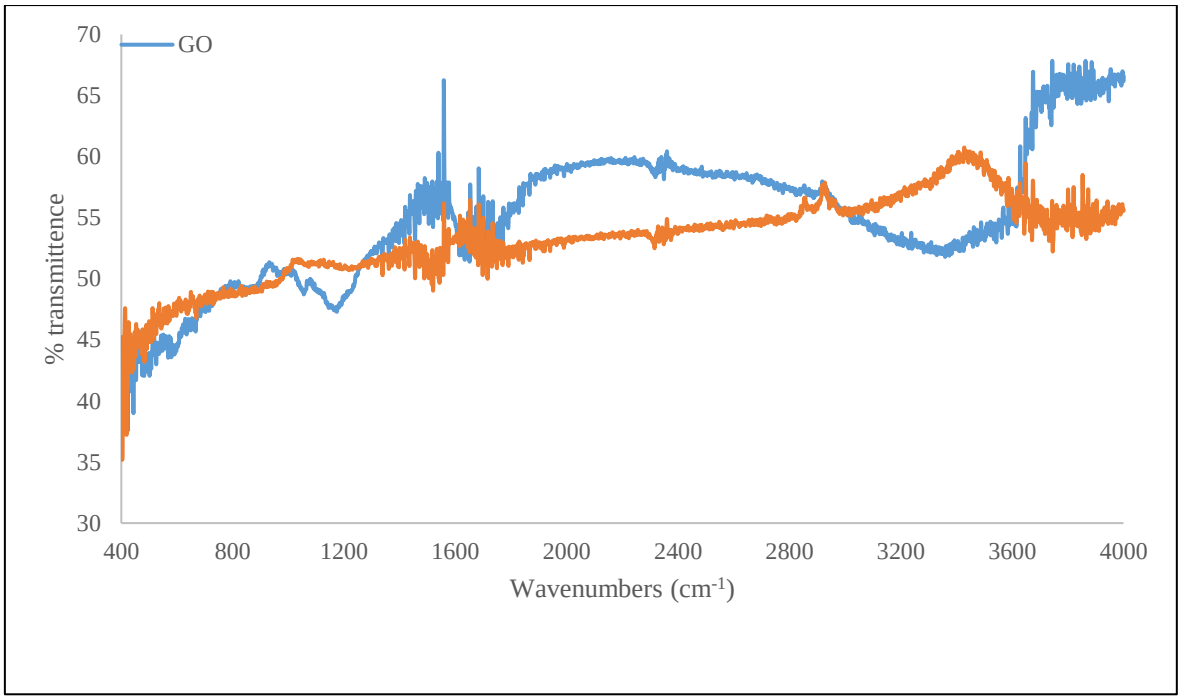

Figure 4 Raman spectra of GO and RGO

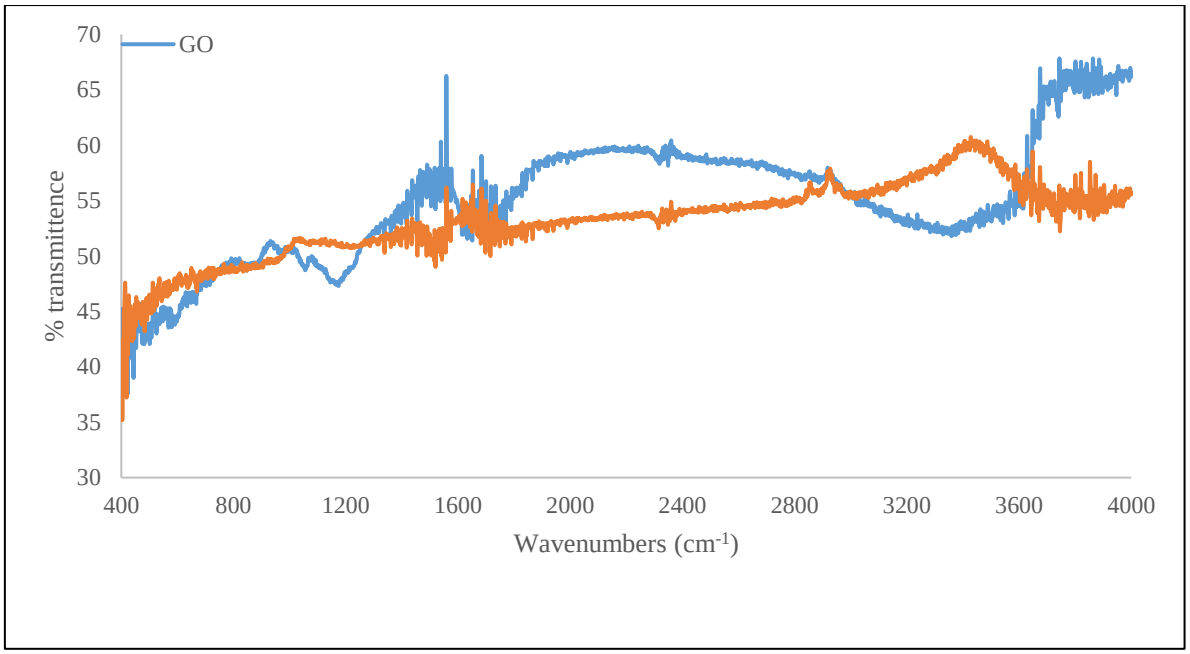

Figure 5 FTIR spectra of GO and RGO

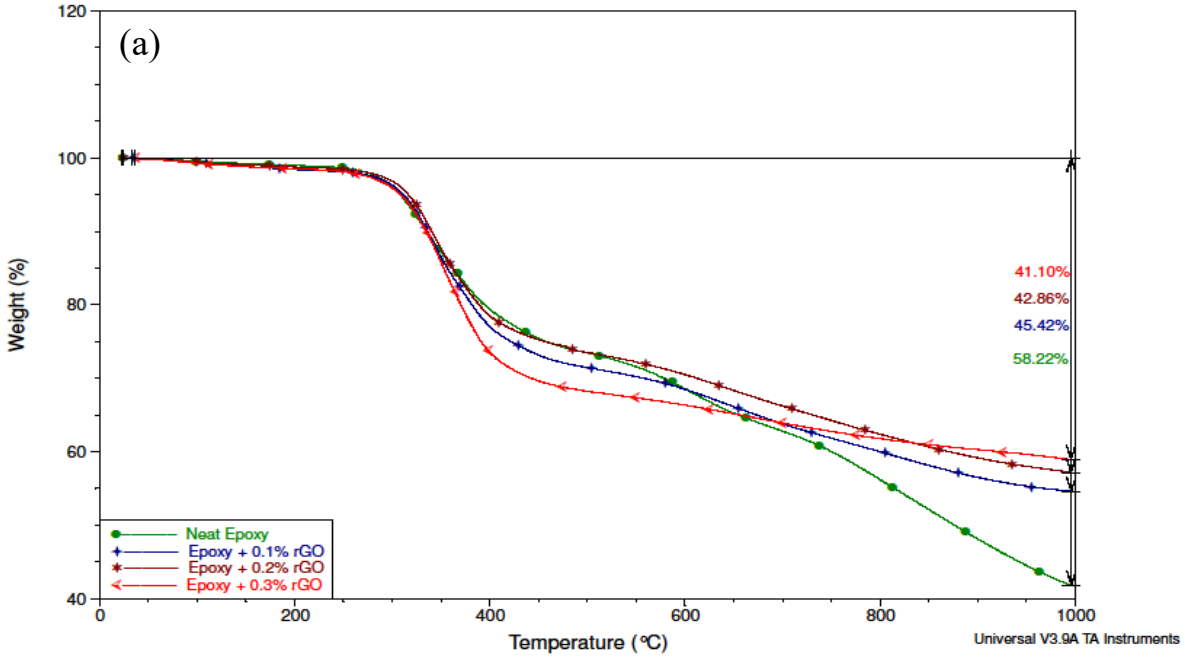
(a)
Weight (%)
Temperature (°C)
Neat Epoxy
Epoxy + 0.1% rGO
Epoxy + 0.2% rGO
Epoxy + 0.3% rGO
41.10%
42.86%
45.42%
58.22%
Universal V3.9A TA Instruments

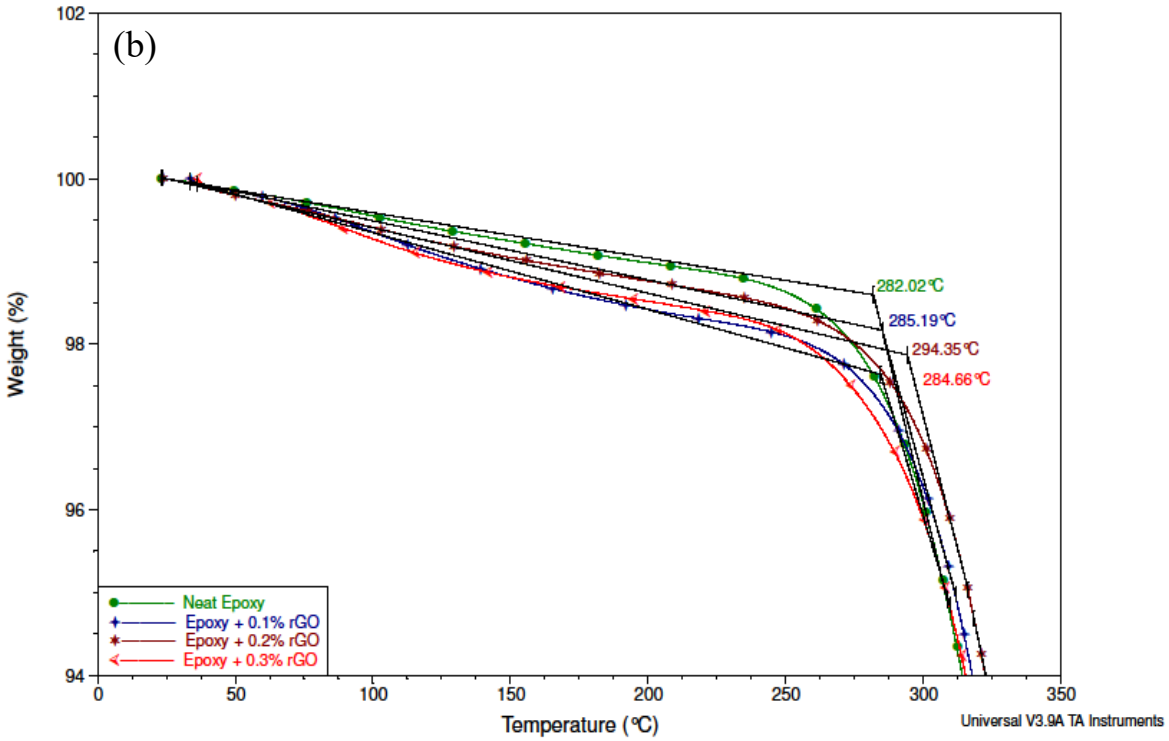
(b)
Weight (%)
Temperature (°C)
Neat Epoxy
Epoxy + 0.1% rGO
Epoxy + 0.2% rGO
Epoxy + 0.3% rGO
282.02°C
285.19°C
294.35°C
284.66°C
Universal V3.9A TA Instruments

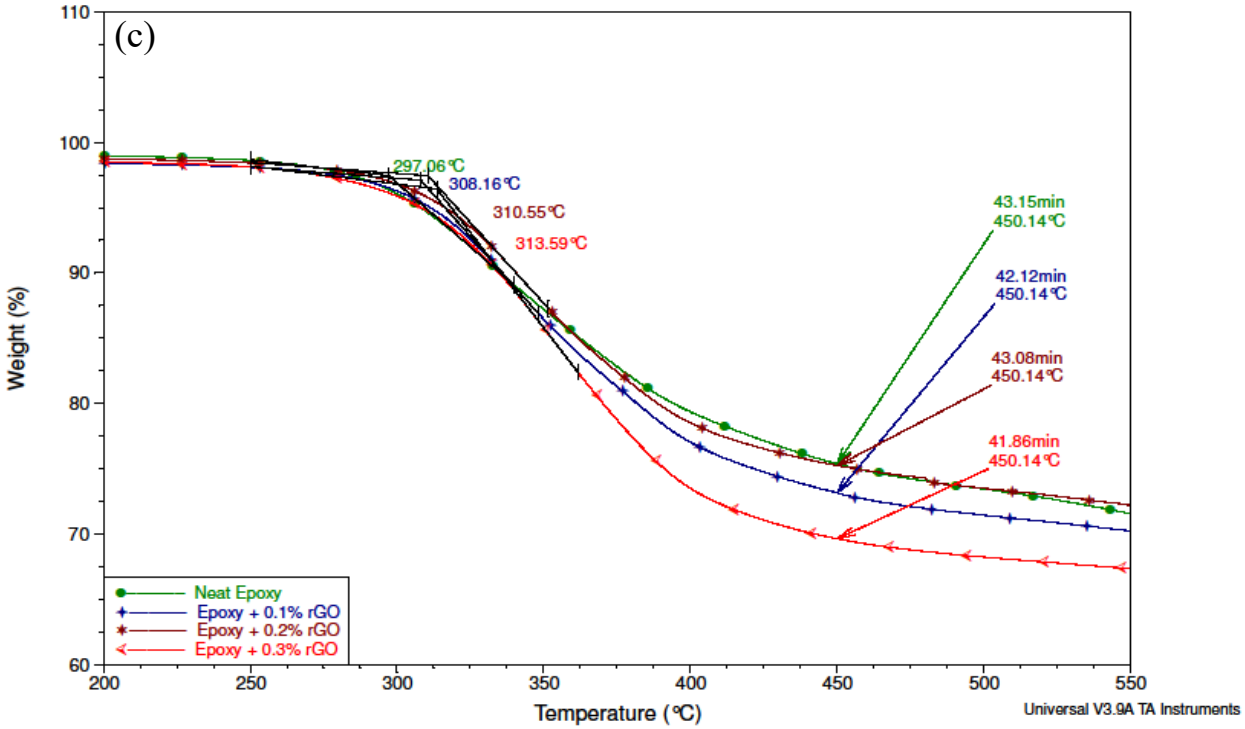

Figure 6 Thermogravimetry results for rGO samples investigated: (a) decomposition thermograms at 1000° C; (b) onset degradation at 5 wt% loss and (c) onset degradation between 250 and 450° C

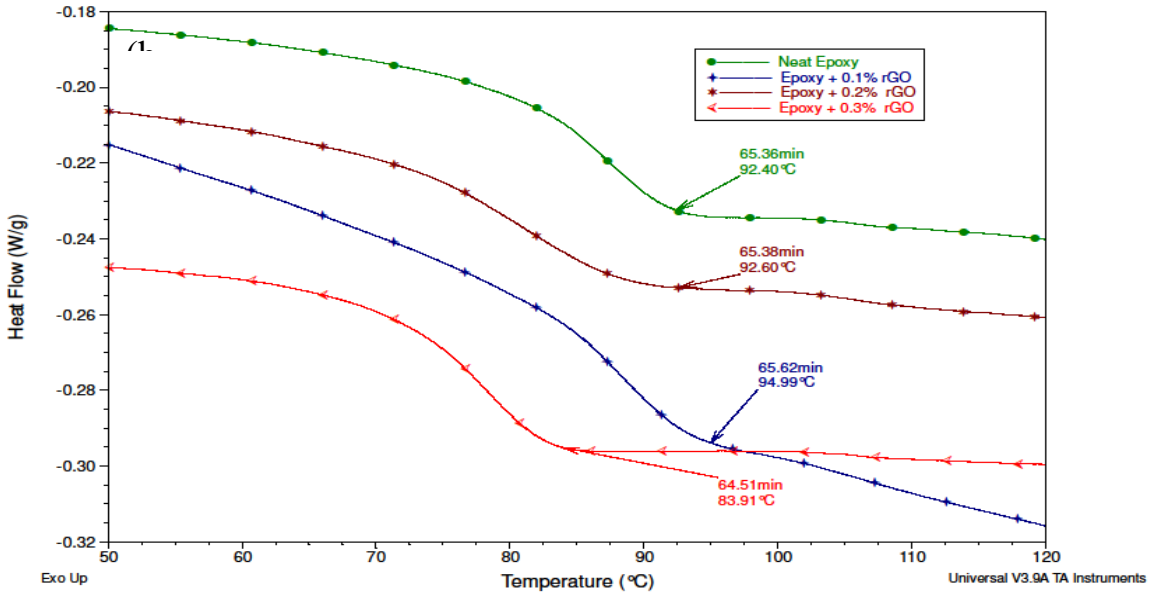

Figure 7 (a) Tg and (b) T_m profiles for rGO samples studie

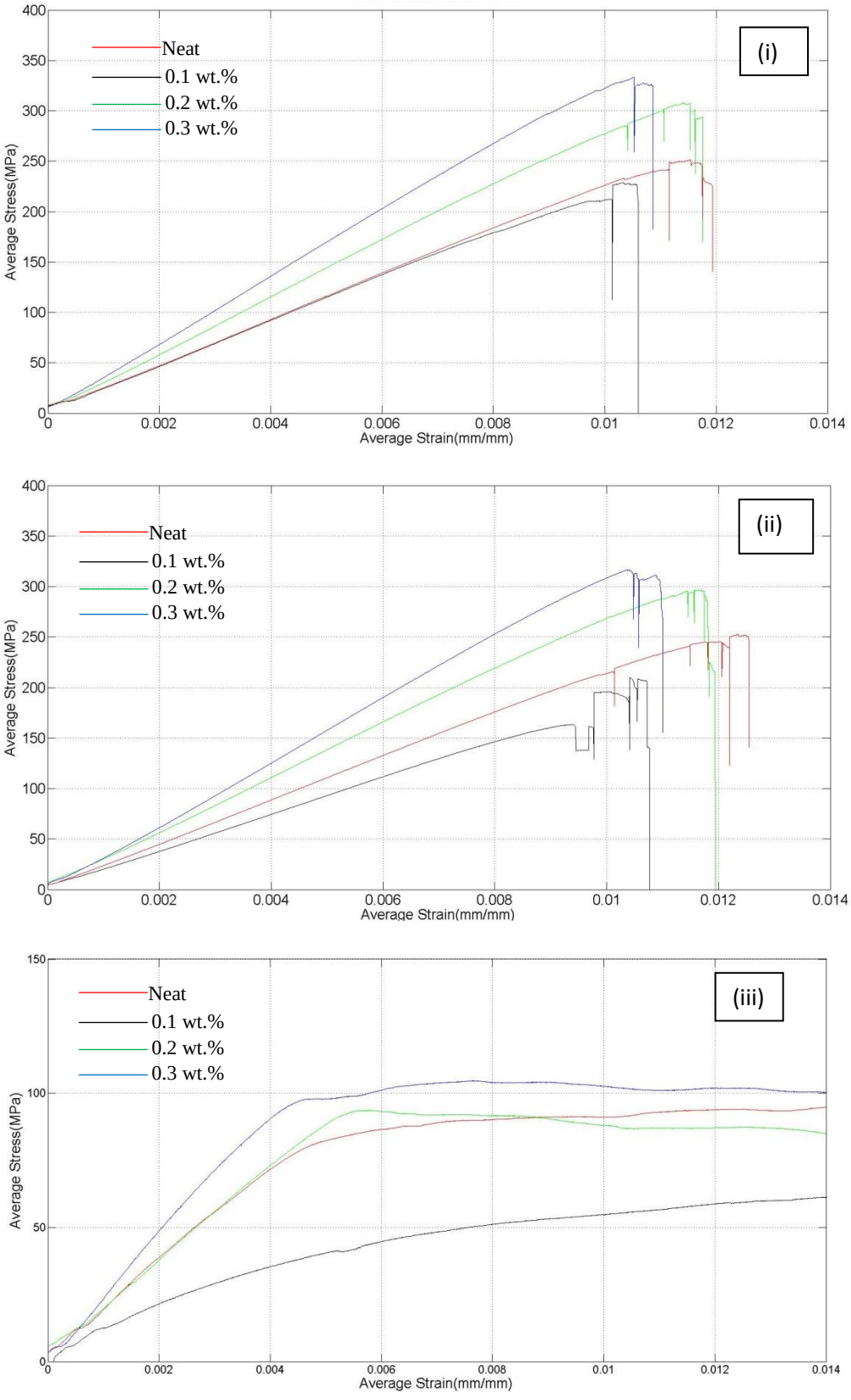

Figure 8 Flexural properties at -10°C (i), at room temperature (ii) and at 40°C (iii).

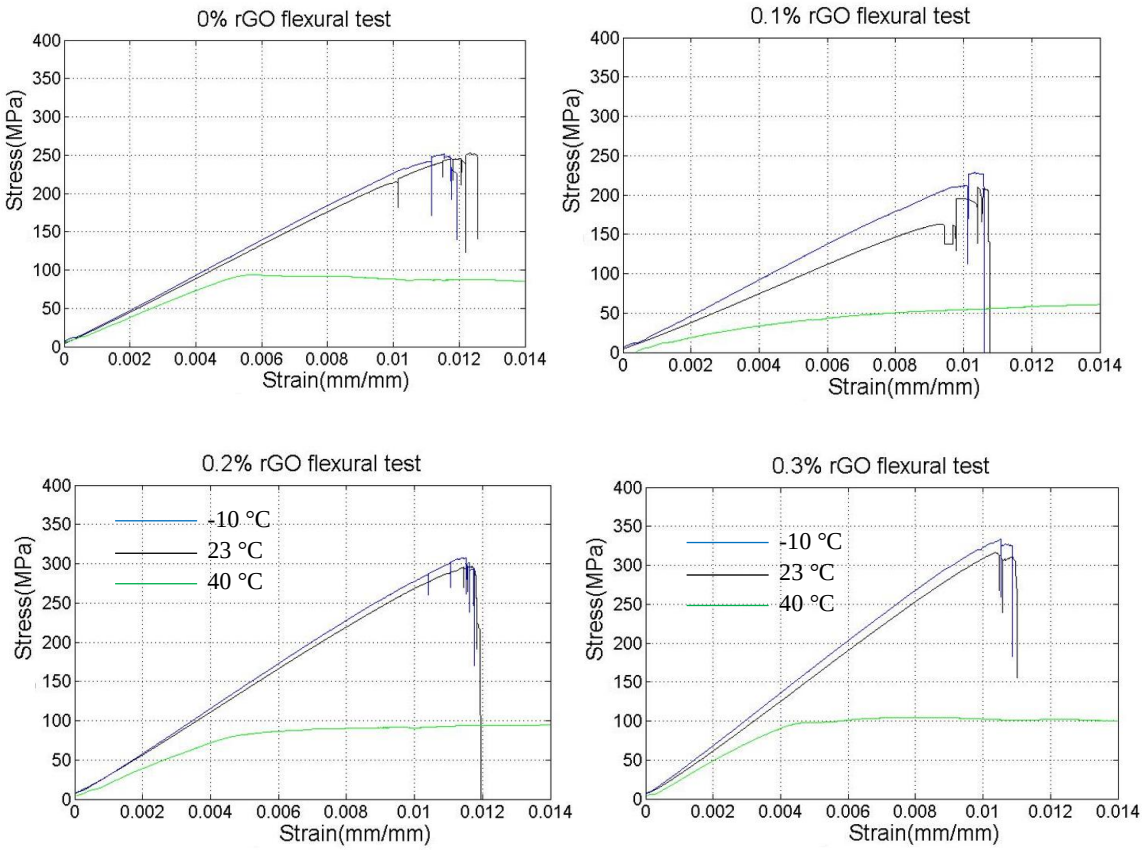

Figure 9 The flexural strength property at various temperatures for studied epoxy/carbon fibre reinforced composites reinforced with 0, 0.1, 0.2, and 0.3 wt.% rGO

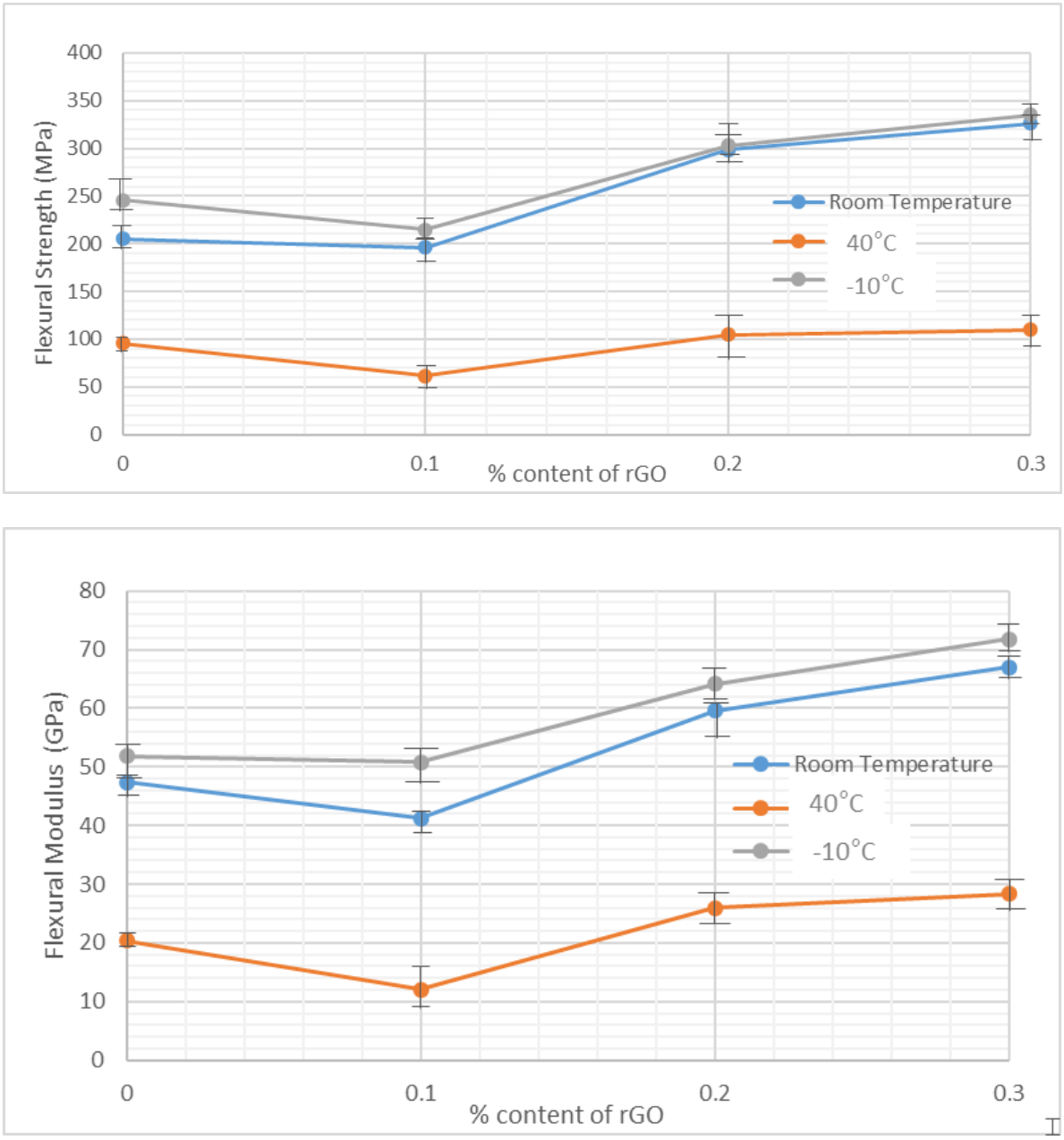

Figure 10 The flexural strength and modulus for studied epoxy/carbon fibre reinforced composites reinforced with 0, 0.1, 0.2, and 0.3 wt.% rGO

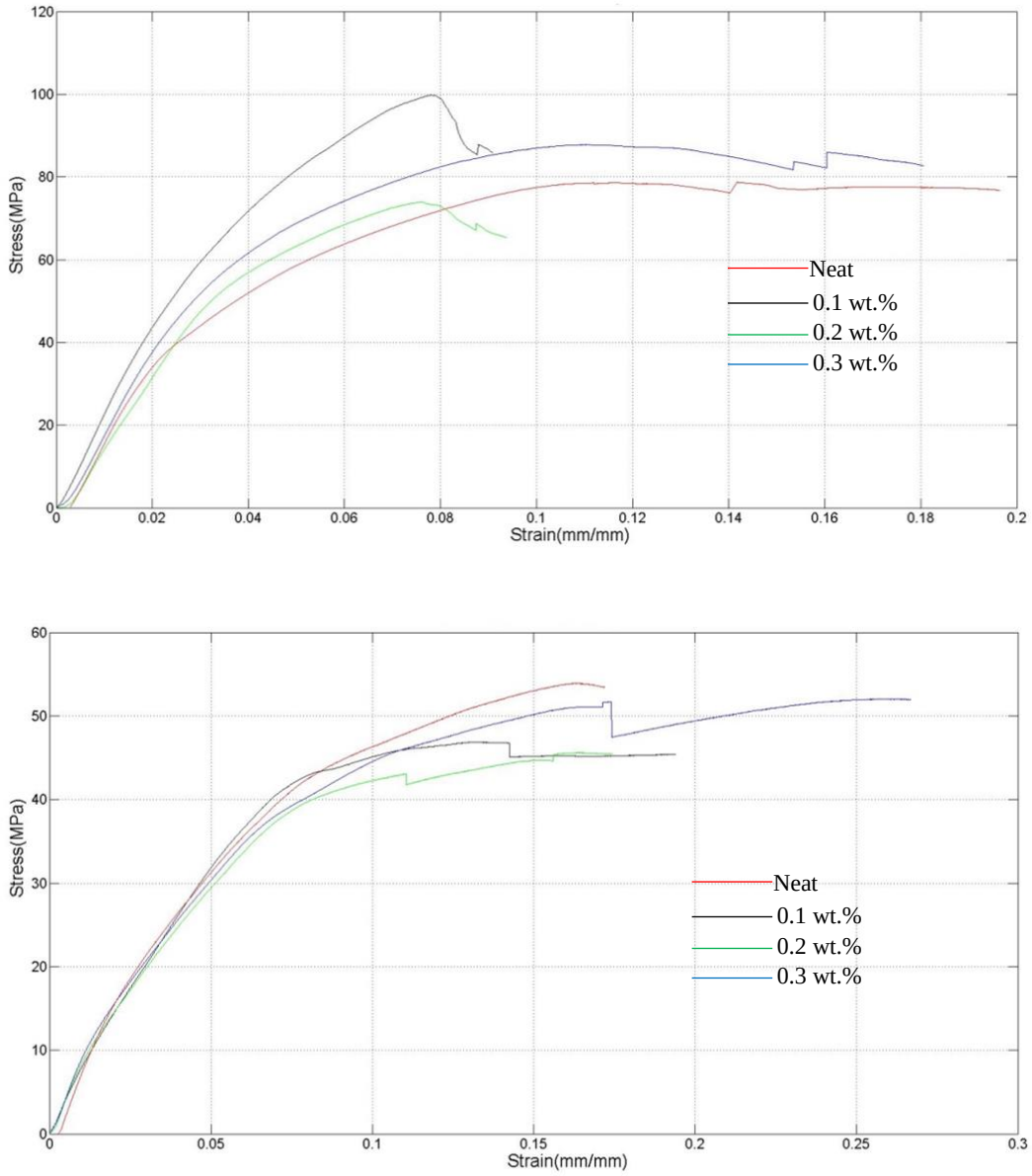

Figure 11 The shear properties at room temperature (top) and at 40 ^{o}C for composites studied.

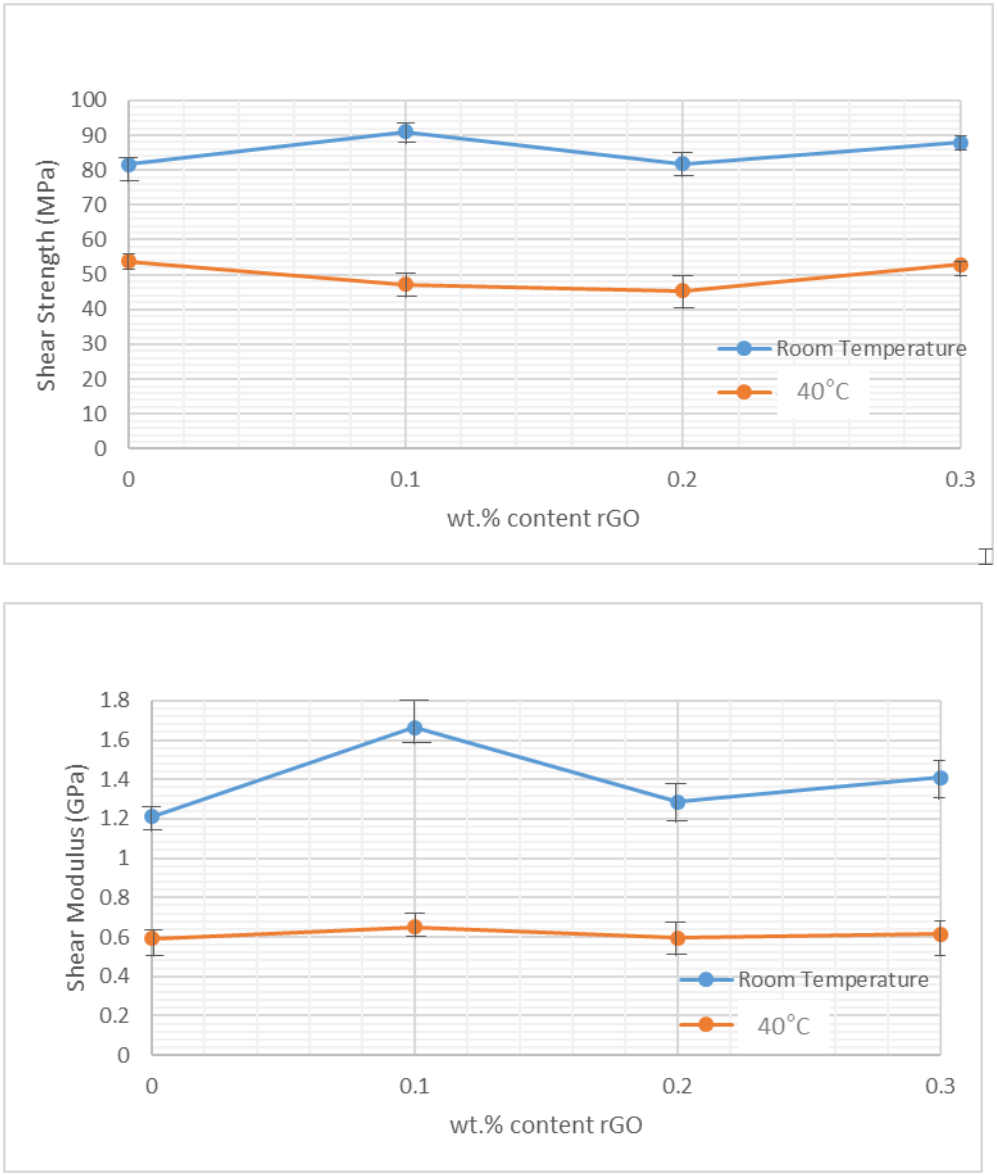

Figure 12 The comparison of shear strength (top) and shear modulus (below) for composites studied.

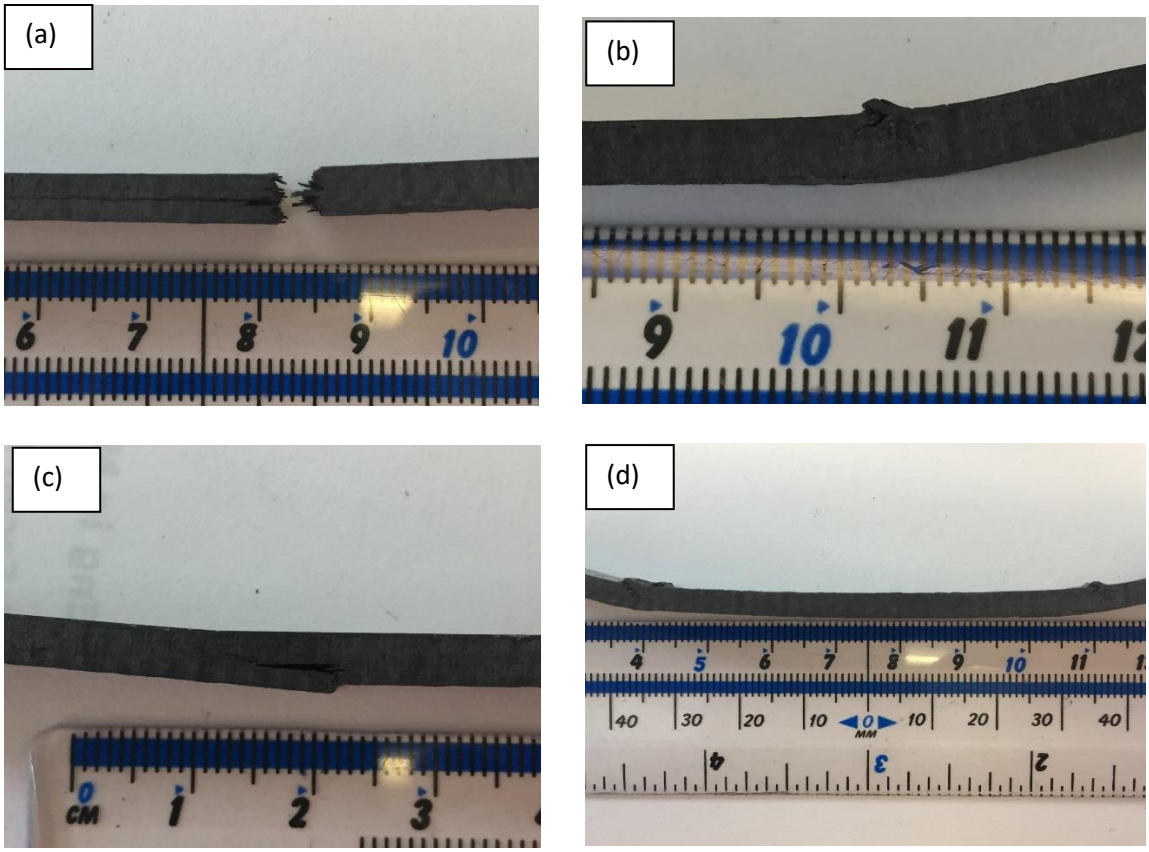

Figure 13 Comparison of damage to reference (neat) flexural samples at cold temperature (a) and hot temperature (b) and those of 0.3 wt.% rGO samples for flexural cold sample (c) and deformed hot sample (d).

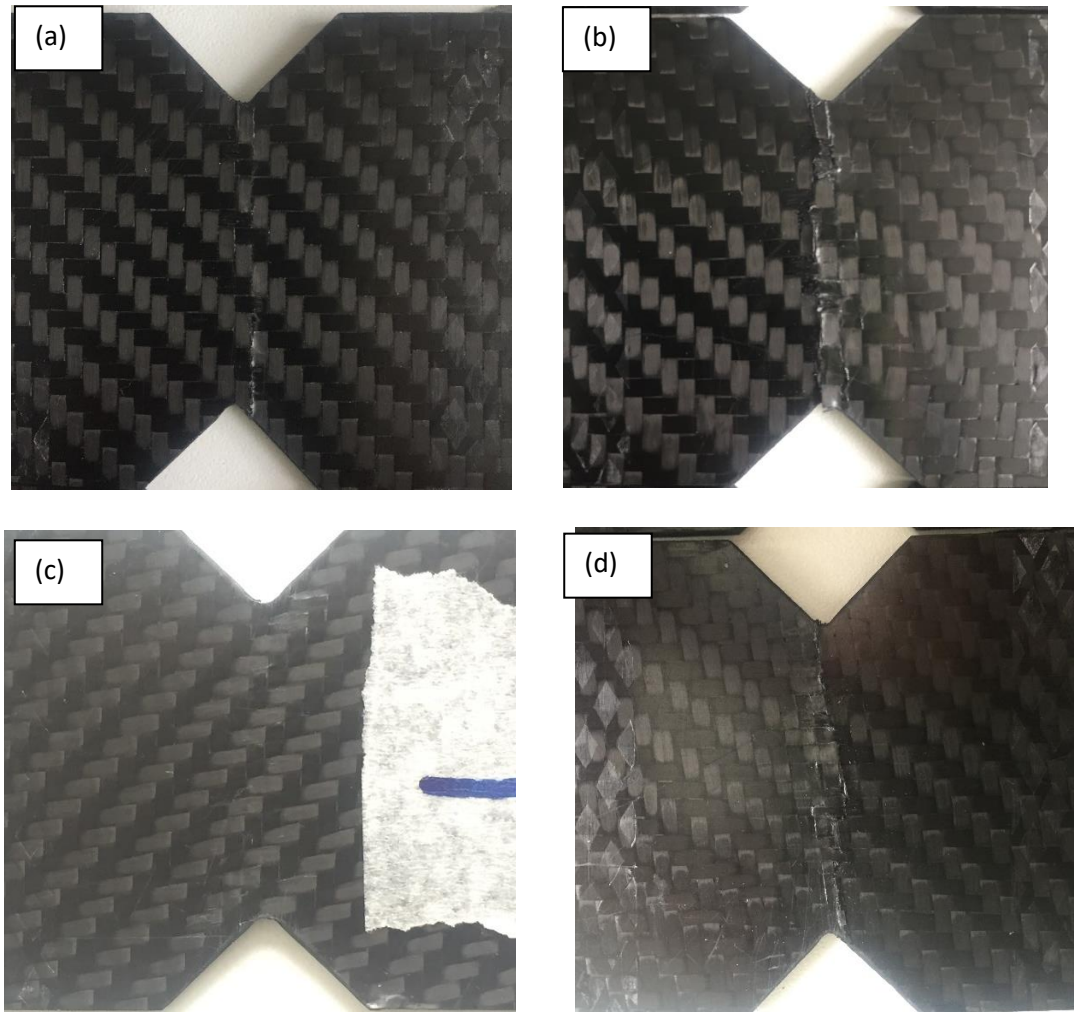

Figure 14 Failure on various shear 0.1 wt.% rGO samples (a) and 0.3 wt.% rGO samples at room temperatures; 0.1 wt.% rGO samples (c) and 0.3 wt.% rGO samples at hot temperature of 40 ^{o}C

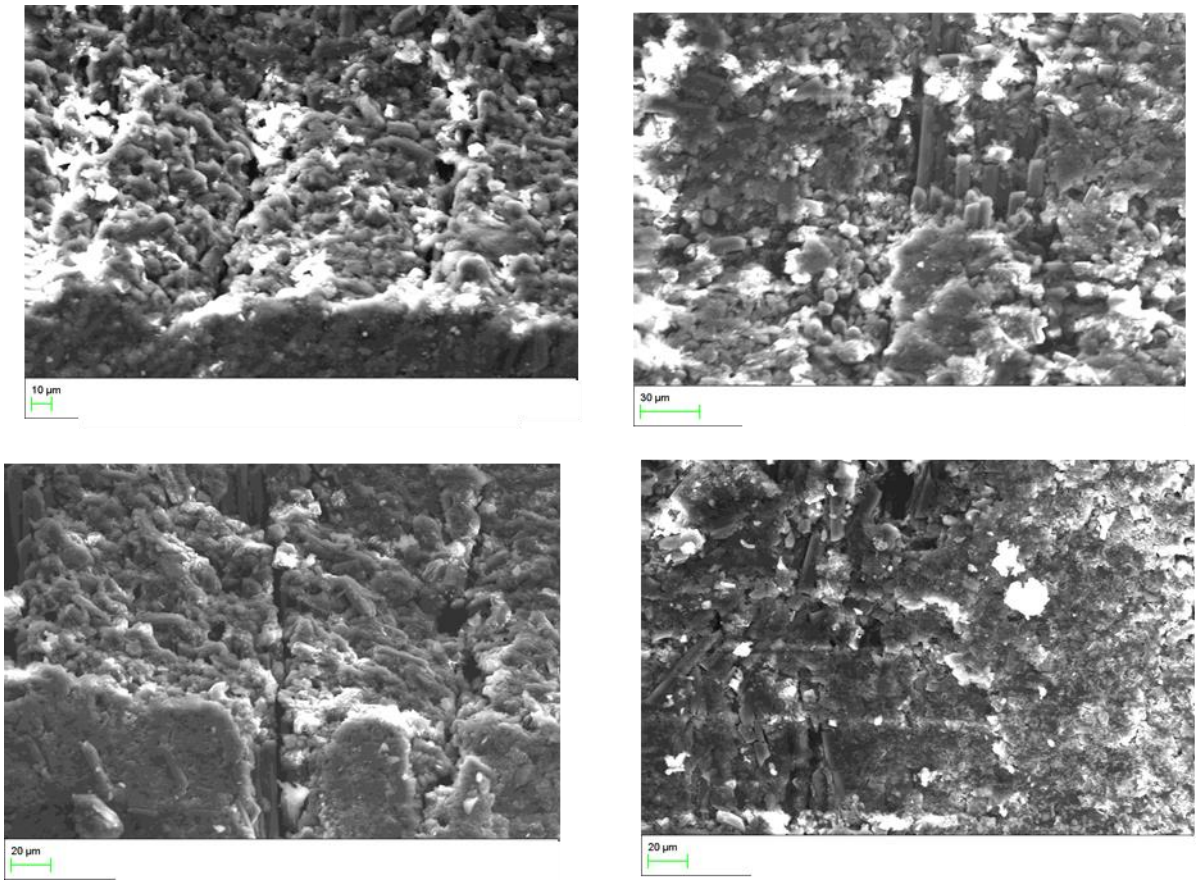

Figure 155 SEM Micrographs of neat (a), 0.1 wt.% rGO (b); 0.2 wt.% rGO (c) and 0.3 wt.% rGO shear composites samples studied